

EFFECTS OF MULTI-CIRCULAR JET PLATES ON THE SPRAY AND FLAME  
CHARACTERISTICS OF INTERNAL MIXING AIR-ASSISTED ATOMIZER

SHHRIN HISHAM BIN AMIRNORDIN

A thesis submitted in  
fulfillment of the requirement for the award of the  
Doctor of Philosophy

Faculty of Mechanical and Manufacturing Engineering  
Universiti Tun Hussein Onn Malaysia

JULY 2020

## ACKNOWLEDGEMENT

I would like to express my gratitude to all those who gave me the possibility to complete this thesis especially to my supervisor, Associate Professor Ts. Dr. Amir bin Khalid who has trusted me on this title and kindly guide me to complete this research. Special thanks to my co-supervisor, Associate Professor Dr. Mas Fawzi bin Mohd Ali who has given motivation and support especially in the research process, data analysis and the writing process. I would like to show my sincere gratitude for those who have contributed directly and indirectly towards the success of this research project. I am deeply indebted to all my colleagues and friends whose help, stimulating suggestions and encouragement helped me in my research work. I also want to thank to all my final year project students and UTHM Falcons basketballers for all their help and support throughout the study.

Especially, I would like to give my special thanks to my wife Hamimah binti Abd Rahman for her love, understanding and wisdom inspired my work; my children, Muhammad Firdaus and Muhammad Amir Faisal; my parents, Amirnordin bin Hasan and the late of Kalsom binti Bahari; the late of parents-in-law and family members whose patience and support enabled me to complete this work.

## ABSTRACT

The mixing of fuel and air plays a major role in the spray and flame behaviour, hence, affects the combustion performance and emissions of the internal mixing air-assisted atomizers. This research aims to determine the effects of multi-circular jet (MCJ) plates on the spray behavior and flame characteristics of air assisted atomizers. The MCJ plates provide the primary air entrance into the mixing chamber. The plates are represented by P1, P2, and P3 characterized by the difference in the open area ratio at 17.8, 18.4 and 18.9 respectively. Additionally, P1, P4, and P5 are represented by the jet-hole angles at 0°, 30° and 45°. In the experiments, the spray and flame images of all plates are captured at equivalence ratios of 0.8 to 1.2 using a Digital Single Lens Reflect camera. The flame temperatures are measured using the infra-red imaging technique while the emissions, burning chamber and stack temperature are also recorded using an emission gas analyzer and K-type thermocouples respectively. Then the computational work is conducted by using ANSYS Fluent to visualize the impact of plate geometry on the internal fluid flow and spray structure. Further analysis using both experiments and simulations have been carried out in order to compare between the P5 configuration and swirl. Results show that a decrease in open area ratio and jet-hole angle increases the flame temperature up to 11.4% and 13.8% respectively. The inclined jet-hole also increases the velocity up to 47.7% and turbulence kinetic energy up to 62.4% in the mixing chamber. In comparison between MCJ plate (P5) and swirl, P5 produces 33.8% lower backpressure but produces higher flame temperature at 4.3%. The result indicates that the MCJ plates are more effective in controlling the spray and flame characteristics of the atomizer. The outcome of this work provides a deeper understanding on the relations of geometry and fuel-air mixing to the characteristics of the internal mixing air-assisted atomizer which will lead to the improvement of burner systems in the future.

## ABSTRAK

Campuran udara dan bahanapi memainkan peranan yang penting terhadap ciri-ciri semburan dan pembakaran, seterusnya mempengaruhi prestasi pembakaran dan gas keluaran pengabut terbantu udara jenis campuran dalaman. Kajian ini menentukan kemampuan kawalan geometri plet pelbagai jet bulatan (MCJ) terhadap ciri-ciri semburan dan pembakaran sebuah pengabut terbantu udara. P1, P2 dan P3 mewakili nisbah kawasan terbuka iaitu 17.8, 18.4 dan 18.9. P1, P4 dan P5 pula mewakili sudut condong kemasukan udara pada  $0^\circ$ ,  $30^\circ$  dan  $45^\circ$ . Di dalam eksperimen, imej semburan dan api kesemua plet diperolehi pada nisbah kesetaraan dari 0.8 hingga 1.2 menggunakan kamera Digital Lensa Tunggal Refleksi. Suhu api diukur menggunakan kaedah pengimejan infra merah manakala gas pelepasan, suhu kebuk pembakaran dan suhu pelepasan gas masing-masing menggunakan penganalisa gas pelepasan dan penyukat suhu jenis-K. Simulasi menggunakan perisian ANSYS Fluent digunakan untuk mendapatkan gambaran terperinci kesan perubahan geometri plet terhadap aliran bendalir dan struktur semburan. Seterusnya analisa menggunakan eksperimen dan simulasi dijalankan untuk membandingkan plet P5 dan pemusar. Keputusan menunjukkan pengurangan nisbah kawasan terbuka dan sudut lubang udara masing-masing meningkatkan suhu api kepada 11.4% dan 13.8%. Sudut lubang udara pula dapat meningkatkan halaju sebanyak 47.7% dan tenaga kinetik gelora sebanyak 62.4% di dalam kebuk campuran. Perbandingan antara plet MCJ (P5) dan pemusar menunjukkan P5 menghasilkan tekanan balik yang lebih rendah sebanyak 33.8% tetapi menghasilkan suhu api yang lebih tinggi sebanyak 4.3%. Ini menunjukkan plet MCJ berkesan untuk mengawal ciri-ciri semburan dan api sesebuah pengabut. Hasil dapatan kajian ini membolehkan pemahaman lebih mendalam antara hubungan geometri dan campuran udara bahanapi terhadap ciri-ciri pengabut terbantu udara jenis campuran dalaman yang boleh menyumbang kepada penambahbaikan sistem pembakaran pada masa hadapan.

## CONTENTS

	<b>TITLE</b>	<b>i</b>
	<b>DECLARATION</b>	<b>ii</b>
	<b>ACKNOWLEDGEMENT</b>	<b>iii</b>
	<b>ABSTRACT</b>	<b>iv</b>
	<b>ABSTRAK</b>	<b>v</b>
	<b>CONTENTS</b>	<b>vi</b>
	<b>LIST OF TABLES</b>	<b>x</b>
	<b>LIST OF FIGURES</b>	<b>xii</b>
	<b>LIST OF SYMBOLS AND ABBREVIATIONS</b>	<b>xviii</b>
	<b>LIST OF APPENDICES</b>	<b>xx</b>
<b>CHAPTER 1</b>	<b>INTRODUCTION</b>	<b>1</b>
	1.1 Background of study	1
	1.2 Problem statement	4
	1.3 Research questions	5
	1.4 Aims	5
	1.5 Objectives	5
	1.6 Research scope	5
	1.7 Novelty of study	6
	1.8 Preview of thesis	7
<b>CHAPTER 2</b>	<b>LITERATURE REVIEW</b>	<b>9</b>
	2.1 Introduction	9
	2.2 Diesel fuel properties	9
	2.3 Atomization	12

2.4	Atomizers	12
2.5	Experimental studies	17
2.5.1	Spray penetration	17
2.5.2	Drop size	18
2.5.3	Pressure drop	34
2.5.4	Spray cone angle	34
2.5.5	Internal mixing	38
2.5.6	Turbulence generators	40
2.5.7	Spray combustion and emission	40
2.6	Computational Fluid Dynamics (CFD) studies	44
2.7	Summary	46
<b>CHAPTER 3 METHODOLOGY</b>		<b>47</b>
3.1	Introduction	47
3.2	Experimental set-up	49
3.2.1	Spray chamber	49
3.2.2	Burning chamber	50
3.2.3	Fuel delivery system	51
3.2.4	Flow rate measurement	53
3.2.5	Diesel fuel	53
3.2.6	Air-assisted atomizer and turbulence generators	54
3.3	Testing and instrumentation	57
3.3.1	Spray imaging	57
3.3.2	Flame visualization	58
3.3.3	Thermal imaging	59
3.3.4	Temperature measurement	59
3.3.5	Emission measurement	59
3.4	Experimental parameters	60
3.4.1	Mass flow rate of air	60
3.4.2	Stoichiometric equation	62
3.4.3	Calculation of the molecular weight of air and diesel fuel	63
3.4.4	Ratio of air and fuel stoichiometry	64

3.4.5	Calculation of the mass flow rate of fuel for experiments (real)	64
3.5	Experimental procedure	65
3.5.1	Air-fuel equivalence ratio (ER)	66
3.5.2	Geometry of multi-circular jet (MCJ) plates	66
3.5.3	Image processing technique	67
3.5.4	Uncertainties in the measurement	68
3.6	Computational Fluid Dynamics (CFD)	69
3.6.1	Computational domain	70
3.6.2	Simulations	74
3.7	Test matrix	75
3.8	Grid independence test	78
3.9	Experimental validation	79
3.10	Summary	82
<b>CHAPTER 4 RESULTS AND DISCUSSIONS</b>		<b>84</b>
4.1	Introduction	84
4.2	Experimental analysis	84
4.2.1	Spray of single-hole nozzle	87
4.2.1.1	Results of observation	89
4.2.1.2	Effects of equivalence ratio (ER) and geometry	92
4.2.2	Spray of multi-hole nozzle	96
4.2.2.1	Results of observation	96
4.2.2.2	Effects of equivalence ratio (ER) and geometry	98
4.2.3	Flame	102
4.2.3.1	Results of observation	102
4.2.3.2	Effects of equivalence ratio (ER) and geometry	104
4.2.4	Flame temperature	108
4.2.4.1	Results of observation	108

4.2.4.2	Effects of equivalence ratio (ER) and geometry	110
4.2.5	Emission	111
4.2.6	Chamber and flue gas temperature	118
4.3	Computational analysis	120
4.3.1	Flow analysis for MCJ plate	121
4.3.2	Effects of open area ratio on the flow behaviour and spray structure	126
4.3.3	Effects of jet-hole angle on the flow behaviour and spray structure	133
4.4	Comparison of spray and flame between MCJ and swirl plates	139
4.4.1	Comparison by experimental analysis	139
4.4.2	Comparison by computational analysis	143
4.5	Summary	151
<b>CHAPTER 5</b>	<b>CONCLUSIONS</b>	<b>152</b>
5.1	Summary of work	152
5.2	Conclusions	152
5.3	Recommendation	154
	<b>REFERENCES</b>	<b>155</b>
	<b>APPENDICES</b>	<b>161</b>



## LIST OF TABLES

2.1	Chemical properties of diesel fuel	10
2.2	Relationship of diesel fuel properties to composition and performance property	11
2.3	Summary of atomizer's performance	33
2.4	Exemplary values of $D_{mean}$ and $\sigma$ and Sauter mean diameters	34
2.5	Two-phase flow regimes inside mixing chamber at (a) constant pressure, increasing GLR (b) constant GLR, increasing pressure	39
3.1	Flow meters	53
3.2	Specification of turbo diesel Euro 5	53
3.3	Plate diagram	56
3.4	Plate specifications	57
3.5	Temperature points	59
3.6	Parameters for primary air	60
3.7	Parameters for secondary air	61
3.8	Mass flow rate of diesel fuel for the experiment	65
3.9	Geometries of atomizer: effects of OA	67
3.10	Geometries of atomizer: effects of jet-hole angle	67
3.11	Summary of boundary conditions	73
3.12	Input value of diesel fuel and air mass flow rate at the atomizer inlet	74
3.13	Experimental conditions	76
3.14	Measurement of single-hole nozzle spray	76
3.15	Measurement of multi-hole nozzle spray	76

3.16	Measurement of multi-hole nozzle flame	77
3.17	Flame temperature	77
3.18	Emissions	77
3.19	Flue gas temperature	77
3.20	Numerical simulations	78
3.21	Simulation parameters	78
3.22	Percentage differences of droplet sizes between experiments and simulations at (a) 20 mm and (b) 30 mm	82
4.1	Experimental parameters	85
4.2	Image analysis and parameters	86
4.3	Thermal images of flame from multi-hole nozzle	109



## LIST OF FIGURES

1.1	Energy outlook around the world (a) Energy consumption by sector and (b) Energy-related carbon dioxide emissions by sector	2
1.2	Twin-fluid atomizers	3
2.1	Properties of sprays and its applications	13
2.2	Pressure atomizer	14
2.3	Rotary atomizer	15
2.4	Structure of air-blast atomizer	16
2.5	Spray penetration against equivalence ratio	18
2.6	Variation of droplet SMD with ALR for different liquid supply pressures	19
2.7	Variation of droplet distribution of parameters with ALR for a constant liquid supply pressure of 103 kPa	20
2.8	Dependence of the droplets SMD on ALR for different air injection areas	22
2.9	Dependence of the liquid flow rate on ALR for different injector lengths	22
2.10	Dependence of the droplets SMD on ALR for different injector lengths	23
2.11	SMD versus GLR for different $\mu$ and $p$ when $x^*=50$ : (a) $p=0.1$ MPa, (b) $p=0.3$ MPa, (c) $p=0.5$ MPa	24
2.12	SMD versus $x^*$ for different $\mu$ : (a) $p = 0.1$ MPa, (b) $p = 0.5$ MPa	24
2.13	Variation of radial velocity distributions for different swirl measured at $z/D_0 = 4.5$	26

2.14	Variation of axial velocity distributions for different swirl	26
2.15	Visualizations of two-phase flow in the internal mixing chamber at various GLR and $p$	27
2.16	SMD change with $p$ and GLR at various $x^*$	28
2.17	SMD change with $p$ and GLR at various $r^*$	29
2.18	Variation of the measured chamber pressure for different liquid and gas flow rates. Air inlet diameter is 4 mm	30
2.19	Internal mixing chamber pressure as a function of the air mass flow rate for a constant water mass flow rate of 950 kg/h and varying air inlet diameter	31
2.20	SMD as a function of air mass flow rate for different air chamber inlet orifice diameters, and a fixed water mass flow rate of 950 kg/h	31
2.21	Liquid breakup regimes (the breakup regimes transitions curves were adapted)	32
2.22	Two-phase flow patterns	32
2.23	Variation of experimentally evaluated $C_d$ with flow rate and comparison with $C_d$ derived from Eqs. 2.1 and 2.2	35
2.24	Behavior of the spray angle ( $2\theta$ ) versus water atomizing pressure	36
2.25	Air liquid mass flow ratio	37
2.26	Shadow graphs at nozzle exit for air flow rates	37
2.27	Influence of the slant of the liquid ports on the SMD	39
2.28	Flue gas temperature profiles along centrelines of the burners	42
2.29	Flue gas temperature of different excess air coefficient (a) $q=1.2$ , (b) $q=1.5$	42
2.30	Comparison of the temperature and soot volume fraction profiles at flame height (a) $z = 30$ mm and (b) $z = 50$ mm	43

3.1	Research flow chart	48
3.2	Image of spray chamber	49
3.3	Image of burning chamber	50
3.4	Schematic diagram of experimental setup	52
3.5	Nozzle geometry	54
3.6	Assembly of air-assisted atomizer	55
3.7	Meshing of spray domain	71
3.8	Bottom view of meshing for atomizer connected with spray chamber	72
3.9	Grid independence study of P1	79
3.10	Spray image of P1	80
3.11	Image analysis at (a) 20 mm from the nozzle for P1 (b) 30 mm from the nozzle for P1	80
3.12	Validation (a) 20 mm (b) 30 mm	81
4.1	Spray from single-hole nozzle of P5 at ER 1.0	88
4.2	Spray from single-hole nozzle of P1	90
4.3	Spray from single-hole nozzle of P2	90
4.4	Spray from single hole nozzle of P3	91
4.5	Spray from single hole nozzle of P4	91
4.6	Spray from single hole nozzle of P5	92
4.7	Spray angle of single-hole nozzle for P1, P2 and P3	94
4.8	Spray penetration of single-hole nozzle for P1, P2 and P3	94
4.9	Spray angle of single-hole nozzle for P1, P4 and P5	95
4.10	Spray penetration of single-hole nozzle for P1, P4 and P5	95
4.11	Spray from multi-hole nozzle of P5 at ER 1.0	96
4.12	Spray from multi-hole nozzle of P1	97
4.13	Spray from multi-hole nozzle of P2	97
4.14	Spray from multi-hole nozzle of P3	97
4.15	Spray from multi-hole nozzle of P4	97
4.16	Spray from multi-hole nozzle of P5	98

4.17	Breakup length of multi-hole nozzle for P1, P2 and P3	100
4.18	Spray angle of multi-hole nozzle for P1, P2 and P3	100
4.19	Breakup length of multi-hole nozzle for P1, P4 and P5	101
4.20	Spray angle of multi-hole nozzle for P1, P4 and P5	101
4.21	Actual flame image from multi-hole nozzle of P5 at ER 1.0	103
4.22	Flame from multi-hole nozzle of P1	103
4.23	Flame from multi-hole nozzle of P2	103
4.24	Flame from multi-hole nozzle of P3	104
4.25	Flame from multi-hole nozzle of P4	104
4.26	Flame from multi-hole nozzle of P5	104
4.27	Flame angle of multi-hole nozzle for P1, P2 and P3	106
4.28	Flame height of multi-hole nozzle for P1, P2 and P3	106
4.29	Flame angle of multi-hole nozzle for P1, P4 and P5	107
4.30	Flame height of multi-hole nozzle for P1, P4 and P5	107
4.31	Thermal image from multi-hole nozzle of P5 at ER 1.0	108
4.32	Flame temperature of multi-hole nozzle for P1, P2 and P3	110
4.33	Flame temperature of multi-hole nozzle for P1, P4 and P5	111
4.34	Emission of multi-hole nozzle combustion for P1, P2 and P3 (a) CO (b) HC (c) CO <sub>2</sub> and (d) O <sub>2</sub>	113
4.35	Emission of multi-hole nozzle combustion for P1, P4 and P5 (a) CO (b) HC (c) CO <sub>2</sub> and (d) O <sub>2</sub>	116
4.36	Chamber temperature of all plates	118
4.37	Stack 1 temperature of all plates	119
4.38	Stack 2 temperature of all plates	120
4.39	Backpressure of P1	122
4.40	Average velocity along the mixing chamber at different fuel flow rates for P1	122

4.41	Turbulence kinetic energy of P1 along the mixing chamber	123
4.42	Velocity streamline and velocity vector of P1	124
4.43	Contour of volume fraction for P1	125
4.44	Volume fraction of P1	125
4.45	Maximum backpressure for P1,P2 and P3	127
4.46	Average velocity of P1, P2 and P3	128
4.47	Turbulence kinetic energy of P1, P2 and P3	128
4.48	Volume fraction of P1, P2 and P3	129
4.49	Droplet density of P1, P2 and P3	131
4.50	SMD of P1, P2 and P3	132
4.51	Maximum backpressure of P1, P4 and P5	134
4.52	Average velocity of P1, P4 and P5	134
4.53	Turbulence kinetic energy of P1, P4 and P5	135
4.54	Volume fraction of P1, P4 and P5	135
4.55	Droplet density of P1, P4 and P5 at (a) 20 mm and (b) 30 mm	137
4.56	SMD of P1, P4 and P5 at (a) 20 mm and (b) 30 mm	138
4.57	Spray angle of single-hole nozzle at 6.17 kg/h	140
4.58	Spray penetration of single-hole nozzle at 6.17 kg/h	140
4.59	Breakup length of multi-hole nozzle at 6.17 kg/h	141
4.60	Spray angle of multi-hole nozzle at 6.17 kg/h	141
4.61	Flame angle of multi-hole nozzle at 6.17 kg/h	142
4.62	Flame height of multi-hole nozzle at 6.17 kg/h	142
4.63	Flame temperature of multi-hole nozzle at 6.17 kg/h	143
4.64	Velocity streamline and velocity vector of (a) MCJ plate and (b) swirl	144
4.65	Maximum backpressure at different mass flow rates	145
4.66	Average velocity of P5 and swirl at 6.17 kg/h	146
4.67	Turbulence kinetic energy of P5 and swirl at 6.17 kg/h	146
4.68	Volume fraction of P5 and swirl at 6.17 kg/h	147
4.69	Spray from P5 and swirl at 6.17 kg/h	148

4.70	Droplets density of P5 and swirl at 6.17 kg/h (a) 20 mm (b) 30 mm downstream of the nozzle	149
4.71	SMD of P5 and swirl at 6.17 kg/h (a) 20 mm (b) 30 mm downstream of the nozzle	150





## LIST OF SYMBOLS AND ABBREVIATIONS

°C	-	Degree celcius
μm	-	Micrometer/Micron
2-D	-	Two-dimensional
3-D	-	Three-dimensional
ALR	-	Air-liquid ratio
ASTM	-	American Society for Testing and Material
CFD	-	Computational Fluid Dynamics
CO	-	Carbon monoxide
CO <sub>2</sub>	-	Carbon dioxide
D, d	-	Diameter
DM	-	Discrete Multicomponent Model
DPM	-	Discrete Phase Models
DSLR	-	Digital single-lens reflex
Eq.	-	Equation
ER	-	Equivalence ratios
fps	-	Frame per second
GLR	-	Gas-liquid ratio
HC	-	Hydrocarbon
kg/h	-	Kilogram per hour
m	-	Meter
mm	-	Milimeter
m/s	-	Meter per second
MCJ	-	Multi-circular jet
MPa	-	Megapascal
MW	-	Molecular weight

N	-	Number of holes
NO <sub>x</sub>	-	Nitrogen oxides
O <sub>2</sub>	-	Oxygen
OA	-	Open area
<i>p</i>	-	pressure
PDF	-	Possibility density function
PM	-	Particulate emissions
ppm	-	Parts per million
<i>Q</i>	-	Flow rate
SMD	-	Sauter mean diameter
TAB	-	Taylor breakup model
TKE	-	Turbulence kinetic energy
<i>V</i>	-	Velocity
$\rho$	-	Density



**LIST OF APPENDICES**

A1	Spray and flame images of swirl	162
A2	Emissions from P5 and swirl	163
A3	Chamber and flue gas temperature for P5 and swirl	166
A4	Specifications of Autocheck Gas & Smoke	168
B	List of publications	169



**PTTA UTHM**  
PERPUSTAKAAN TUNKU TUN AMINAH

## CHAPTER 1

### INTRODUCTION

#### 1.1 Background of study

Combustion has been the foundation of the population and industrial growth around the world for the past centuries. There are six major uses for combustion in the industry which are petroleum refining, chemicals, iron and steel, smelting, pulp and paper, and cement. The burning of fuel to produce heat or other forms of power produces combustion, which is part of the industrial processes. However, a trend related to the energy outlook around the world reveals that for the last 10 years, world energy consumption has shown a steady growth at an average of 1.7% growth. In 2019, energy consumption shows that the industrial sector is in the third highest energy requirement and will move to second place by 2025 (Figure 1.1(a)). In addition, petroleum oil ranks the highest in energy consumption from 2019 until 2050. As a result, the growth in energy consumption contributes to the carbon dioxide emission which shows an average of 1.3% growth rate (Figure 1.1(b)) for the past 10 years and continues to increase in the future (Energy Information Administration, 2020).

The global industrial burner industry is in a phase of transition to factory automation and integration of components. However, the needs for improving operational efficiency and reducing the level of emissions remains a trend in developing countries (Persistent Market Research, 2019). Therefore, burners have been used as the integral parts of boilers and industrial heating systems. The key performance targets of a burner system are divided into three. First is the reduction of nitrogen oxides (NO<sub>x</sub>), carbon monoxide (CO) and particulate emissions (PM).

Second is to maximize system efficiency for reducing carbon dioxide (CO<sub>2</sub>) emissions. Last target is to reduce specific fuel consumption. In the burner system, atomizers are the most important component in mixing both the fuel and oxidizer. The atomizer transforms a certain volume of liquid into sprays or other types of dispersion into small drops in order to increase its surface area. It discharges the liquid at high velocity into a relatively slow-moving stream of air or gases (Mashayek & Ashgriz, 2011).

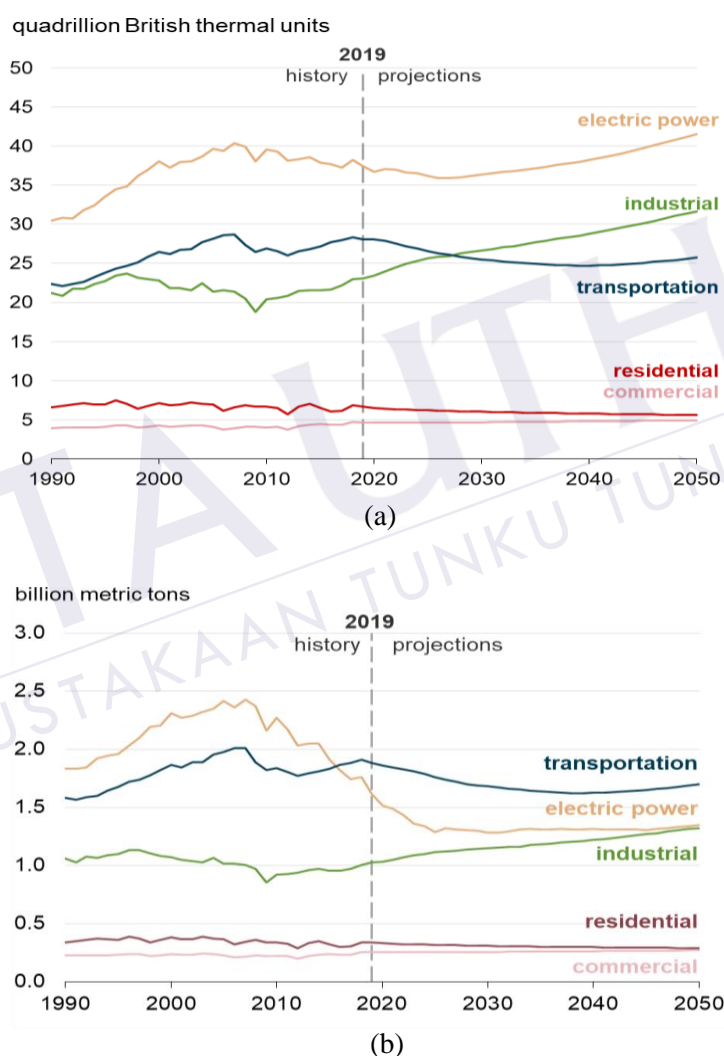


Figure 1.1: Energy outlook around the world (a) Energy consumption by sector and (b) Energy-related carbon dioxide emissions by sector (Energy Information Administration, 2020)

Atomizers are categorized according to their working principles and typical applications. Basically, it requires a high relative velocity between the liquid and the

surrounding air or gases. The first technique involves a discharge of high-velocity liquid into a relatively slow movement of air or gas, i.e. pressure atomizer and rotary atomizer. The second technique involves the relatively slow-moving liquid exposed to high pressure or velocity of air; known as twin-fluid atomization (Figure 1.2). Typical atomizers are included air-blast, effervescent and air-assisted atomizers (Lefebvre & Ballal, 2010).

Air-assisted atomizers are introduced in order to counter the low-pressure differential of a simplex nozzle, which reduces the atomization quality. Inside the atomizer, pressurized air is used to augment the atomization process at the lowest flow rate. Currently, two configurations of air-assisted atomizers are available with different fuel-air mixing mechanism. In external mixing form, high-velocity gas or steam impinges on the liquid, at or outside the liquid discharge orifice; whereas in internal-mixing configurations, air or gas and liquid mix within the nozzle before discharged through the outlet orifice. The liquid and pressurized air sometimes are supplied through tangential slots to encourage fuel and air mixing, which influence the discharge pattern into a conical form, hence affects the combustion characteristics of the atomizer (Lefebvre & McDonell, 2017; Yatsufusa, Kidoguchi & Nakagawa, 2014). As additional, effects of the outlet shape on the spray angle of effervescent-swirl atomizer also has been determined previously. Results show that swirl atomizer produces widest spray angle for the profiled outlet (Ochowiak *et al.*, 2015). In addition, the swirling motion assisting the fuel and air mixing by producing centrifugal forces will result in a vortex formation within the body (Vigueras-Zuniga *et al.*, 2014; Zhang *et al.*, 2017; Wlodarczak, Ochowiak & Matuszak, 2018; Hreiz, Gentric & Midoux, 2011).

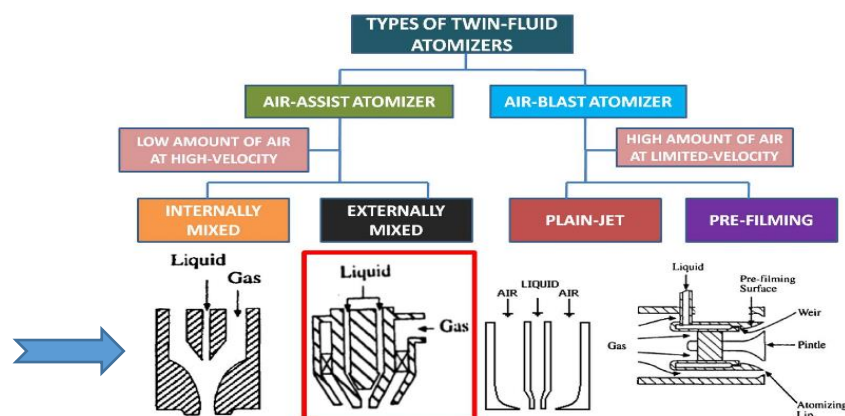


Figure 1.2: Twin-fluid atomizers (Lefebvre & McDonell, 2017)

## 1.2 Problem statement

Burner combustion in industrial applications is highly complex systems due to various complicating factors of heat transfer during combustion, non-uniform size of spray droplets and complex flow and mixing patterns in the mixing chamber or the combustion chamber. The mixing of fuel and oxidizer takes place in the burner chamber, where the mechanics of mixing process play an important role. The mixing is dependent on the geometry, spatial distribution, momentum of the air flow and influence of any flame stabilization devices such as turbulence generators.

Swirl is a type of turbulence generators used in industrial combustion. It produces a predominant flow mechanism effective in controlling the flame stability and combustion intensity. It utilizes swirling motion to generate a recirculation zone for mixing the fuel and oxidizer and generate compact flame with much higher combustion intensity. It characterizes the size and strength of recirculation to determine effects on flame stability and combustion intensity.

The complexity of the recirculation zone produces non-linear characteristics of flame. As a result, it elucidates the responsible basic process for initiating and sustaining combustion instabilities. The development of the passive and active control methodologies for combustion instabilities are substantial in a current research area (Dunn-Rankin, 2008). In order to control the flame characteristics, it requires the controllability of fuel and air mixing by using the geometry of high blockage plates.

Multi-circular jet (MCJ) plates have been identified as a turbulence generation system that yields large turbulent Reynolds numbers in a compact configuration. It allows highly turbulent and reasonably homogeneous flows inside the nozzle. Although numerous studies have been focused on turbulence generators and its effects on the spray and combustion, there is limited literature discussing alternative solutions on the geometry of primary air entrance particularly by using the MCJ plates in the mixing chamber. It is anticipated that this approach has high potential for improving the fuel and air mixing in the atomizers, hence can assist in controlling the spray combustion from the burner (Coppola & Gomez, 2009).

### 1.3 Research questions

In order to address the stated issues, the following questions needs to be resolved.

- (i) How significant is the effect of MCJ plate geometry on the spray and flame characteristics from internally mixed air assisted atomizer?
- (ii) How does the MCJ plate geometry influences the fuel and air mixing and how does it contributes to the spray formation?
- (iii) What the different between MCJ plate and swirl in terms of spray and flame characteristics?

### 1.4 Aims

This research aims to determine the effects of MCJ plates geometrical configurations of primary air entrance on the mixing induced by the two-phase flow of liquid fuel and air inside the mixing chamber of the internal mixing air-assisted atomizer.

### 1.5 Objectives

The specific objectives of this research are:

- (i) To determine the effects of MCJ plates on the geometrical configurations of spray and flame characteristics for the internally mixed air-assisted atomizer.
- (ii) To analyse the internal fluid flow inside the mixing chamber and its relation to the spray structure produced by the two-phase flow of fuel and air.
- (iii) To compare the spray and flame characteristics, together with the fluid flow mechanism and spray structure of one of the MCJ plates with swirl.

### 1.6 Research scope

The scope of the study as follows:

- (i) Internal mixing air-assisted atomizer is used in this study.



## LIST OF PUBLICATIONS

## MAIN AUTHOR

1. **Amirnordin, S. H.**, Khalid, Yaw, V.Y., Fawzi, M., (2019). Effect of jet-hole angle on the spray characteristics of air-assisted atomizer. *Proceedings of Numerical Analysis in Engineering 2019*.
2. Khalid, A., **Amirnordin, S. H.**, Vasuthavan, U., Hariri, A. & Fawzi, M. (2019). Spray formation in the multi-hole nozzle of twin-fluid atomizers, *Journal of Advanced Research in Fluid Mechanics and Thermal Sciences* 1(1), 75–81.
3. Khalid, A., Suardi, M., Chin, R. Y. S., & **Amirnordin, S. H.** (2017). Effect of biodiesel-water-air derived from biodiesel crude palm oil using premix injector and mixture formation in burner combustion. In *Energy Procedia* (Vol. 111).
4. **Amirnordin, S. H.**, Khalid, A., Sapit, A., Manshoor, B., Sahari, M. F., & Fawzi, M. (2017). Spray characteristics of a multi-circular jet plate in an air-assisted atomizer using Schlieren photography. *ARPJ Journal of Engineering and Applied Sciences*, 12(4).
5. **Amirnordin, S. H.**, Khalid, A., Suardi, M., Manshoor, B., & Hushim, M. F. (2017). Effects of fractal grid on spray characteristics and flame development in burner combustion. *Journal of Physics: Conference Series*, 822(1).
6. **Amirnordin, S. H.**, Khalid, A., Igram Patrick, D., Faizal Mohideen Batcha, M., & Fawzi Mohd Ali, M. (2017). Spray and combustion characteristics of a novel multi-circular jet plate in air-assisted atomizer. In *MATEC Web of Conferences* (Vol. 135).
7. **Amirnordin, S. H.**, Khalid, A., Zailan, M. F., Fawzi, M., Salleh, H., & Zaman, I. (2017). Thermal imaging of flame in air-assisted atomizer for burner system. In *IOP Conference Series: Materials Science and Engineering* (Vol. 226).

8. **Amirnordin, S. H.**, Khalid, A., Ismail, I. A., Yii Shi Chin, R., & Fawzi, M. (2016). Flow characteristics of multi-circular jet plate in premix chamber of air-assist atomizer for burner system. In *MATEC Web of Conferences* (Vol. 78).
9. **Amirnordin, S. H.**, Khalid, A., Sapit, A., Salleh, H., Razali, A., & Fawzi, M. (2016). Spray formation of biodiesel-water in air-assisted atomizer using Schlieren photography. In *IOP Conference Series: Materials Science and Engineering* (Vol. 160).
10. Chin, R. Y. S., Khalid, A., Ghani, A. M. A., Issak, M. M., & **Amirnordin, S. H.** (2016). A comparison between the fractal and swirl injector of diesel spray characteristics in the burner system. *ARPN Journal of Engineering and Applied Sciences*, 11(12), 7491–7497.
11. Suardi, M., **Amirnordin, S. H.**, & Khalid, A. (2016). Effect of mixture formation on combustion in burner system. *ARPN Journal of Engineering and Applied Sciences*, 11(12).
12. Suardi, M., Khalid, A., Razali, M. A., Sapit, A., & **Amirnordin, S. H.** (2016). Effects of fractal grid on emissions in burner combustion by using fuel-water-air premix injector derived from biodiesel crude palm oil (CPO) base. In *MATEC Web of Conferences* (Vol. 90).
13. Yii Shi Chin, R., **Amirnordin, S. H.**, Mansor, N., & Khalid, A. (2015). Numerical analysis of nozzle hole shape to the spray characteristics from premix injector in burner system : a review. *Applied Mechanics and Materials*, 773–774, 610–614.
14. Khalid, A., Lambosi, L., Suardi, M., **Amirnordin, S. H.**, Zaman, I., Mansor, N., & Manshoor, B. (2015). Spray characteristic of rapid mixing jatropha oil biodiesel in burner system, *Applied Mechanics and Materials*, 773–774, 496–500.
15. Yii Shi Chin, R., **Amirnordin, S. H.**, & Khalid, A. (2015). Effects of nozzle shape on the flow characteristics of premix injector using Computational Fluid Dynamics (CFD). *Applied Mechanics and Materials*, 773–774, 450–454.
16. Khalid, A., **Amirnordin, S. H.**, Lambosi, L., Manshoor, B., Sies, M. F., & Salleh, H. (2014). Spray characteristic of diesel-water injector for burner system. *Advanced Materials Research* (Vol. 845).

17. Suardi, M., Azman, N., Samsudin, D., **Amirnordin, S. H.**, & Khalid, A. (2014). Effect of mixture formation of biodiesel-water-air rapid mixing derived from crude palm oil and waste cooking oil in burner combustion. *Applied Mechanics and Materials* (Vol. 660).
18. Khalid, A., Lambosi, L., Lokman, M. M., Manshoor, B., Zaman, I., Sapit, A., & **Amirnordin, S. H.** (2014). Effect of biodiesel from waste cooking oil on mixture formation and emission of burner combustion. *Applied Mechanics and Materials* (Vol. 607).
19. **Amirnordin, S. H.**, Ihsanulhadi, N., Alimin, A. J., & Khalid, A. (2013). Effects of palm oil biodiesel blends on the emissions of oil burner. *Applied Mechanics and Materials* (Vol. 315).



PTTA UTHM  
PERPUSTAKAAN TUNKU TUN AMINAH